Relativistic Configuration Interaction Calculations of K_α Satellite Properties for Aluminum Ions

Ping Wang, J.J. MacFarlane, G.A. Moses

September 1992

UWFDM-907

Submitted to Phys. Rev.

FUSION TECHNOLOGY INSTITUTE

UNIVERSITY OF WISCONSIN

MADISON WISCONSIN

Relativistic Configuration Interaction Calculations of Kα Satellite Properties for Aluminum Ions

Ping Wang, Joseph J. MacFarlane, and Gregory A. Moses

Fusion Technology Institute
Department of Nuclear Engineering and Engineering Physics
University of Wisconsin-Madison
Madison, Wisconsin 53706

UWFDM-907

September 1992

Submitted to *Phys. Rev.*

Abstract

Configuration interaction calculations with Breit-Pauli relativistic corrections have been carried out for aluminum ions to study the properties of Kα satellite spectra produced by proton beam heated aluminum plasmas. Detailed calculations have been performed both for transitions involving the ground configuration states and for transitions involving low excited configuration states. Calculated wavelengths for the Kα transitions are compared with a spectrum obtained during a PBFA-II proton beam/plasma interaction experiment. Our calculations show that the Kα satellite lines can be classified into two distinct groups: one involving transitions of type $1s^1 2s^m 2p^n \rightarrow 1s^2 2s^m 2p^{n-1}$, the other $1s^1 2s^m 2p^{n-1} 3l \rightarrow 1s^2 2s^m 2p^{n-2} 3l$. The former gives the 'characteristic' satellite line position of an ion, while the latter overlaps with lines of the next higher ionization stage. The 'overlap' group can significantly affect the observed line shape of the Kα spectra. Examination of correlation effects and relativistic corrections on the Kα transition energies indicates that both corrections are important.

1. Introduction

Kα lines result from transitions between an atomic state having at least one vacancy in the $1s$ shell and a state in which an electron from the $2p$ subshell fills this vacancy. The Kα lines corresponding to transitions from initial states having one hole in the K shell and n holes in the L shell are the satellite Kα lines. These satellite Kα lines are blue-shifted with respect to the principal Kα lines because of the reduced screening of the nucleus which results when there are fewer spectator electrons. In the case of light elements (atomic number Z less than 20), the energy shift (the distance between the consecutive satellites) caused by introducing an additional hole in the L shell is readily observable in present day laboratory plasma experiments ($\Delta\lambda/\lambda \sim 10^{-2}$). It has been suggested that this characteristic of Kα satellite spectra can be used as a temperature diagnostic for plasmas heated by particle beams in inertial fusion experiments [1]. Light-ion impact ionization of K-shell electrons populates autoionizing states, which then produce fluorescence Kα line emission. Since the Kα satellite lines from Ne-like to He-like ions exhibit detectable shifts to shorter wavelengths, Kα satellite line spectra can provide a measure of the ionization distribution in a plasma, and from that, constraints on plasma conditions.

The first spectroscopic observation of Kα x-ray satellite lines in an intense proton beam experiment was recently made during a Particle Beam Fusion Accelerator II (PBFA-II) experiment at Sandia National Laboratories [2]. In this experiment an aluminum target was irradiated with a $4-6$ MeV, $1-2$ TW/cm^2 proton beam. An elliptic crystal spectrograph was used to obtain a time-integrated spectrum (see Figure 1). Two important features should be noted in this experimental Kα satellite spectrum. First, there is a high degree of structure which is likely caused by term-dependent Kα transitions. In addition, the satellite line shapes are very broad. It has been suggested [3] that this broad line shape may come from the overlap of the Kα satellite lines from the

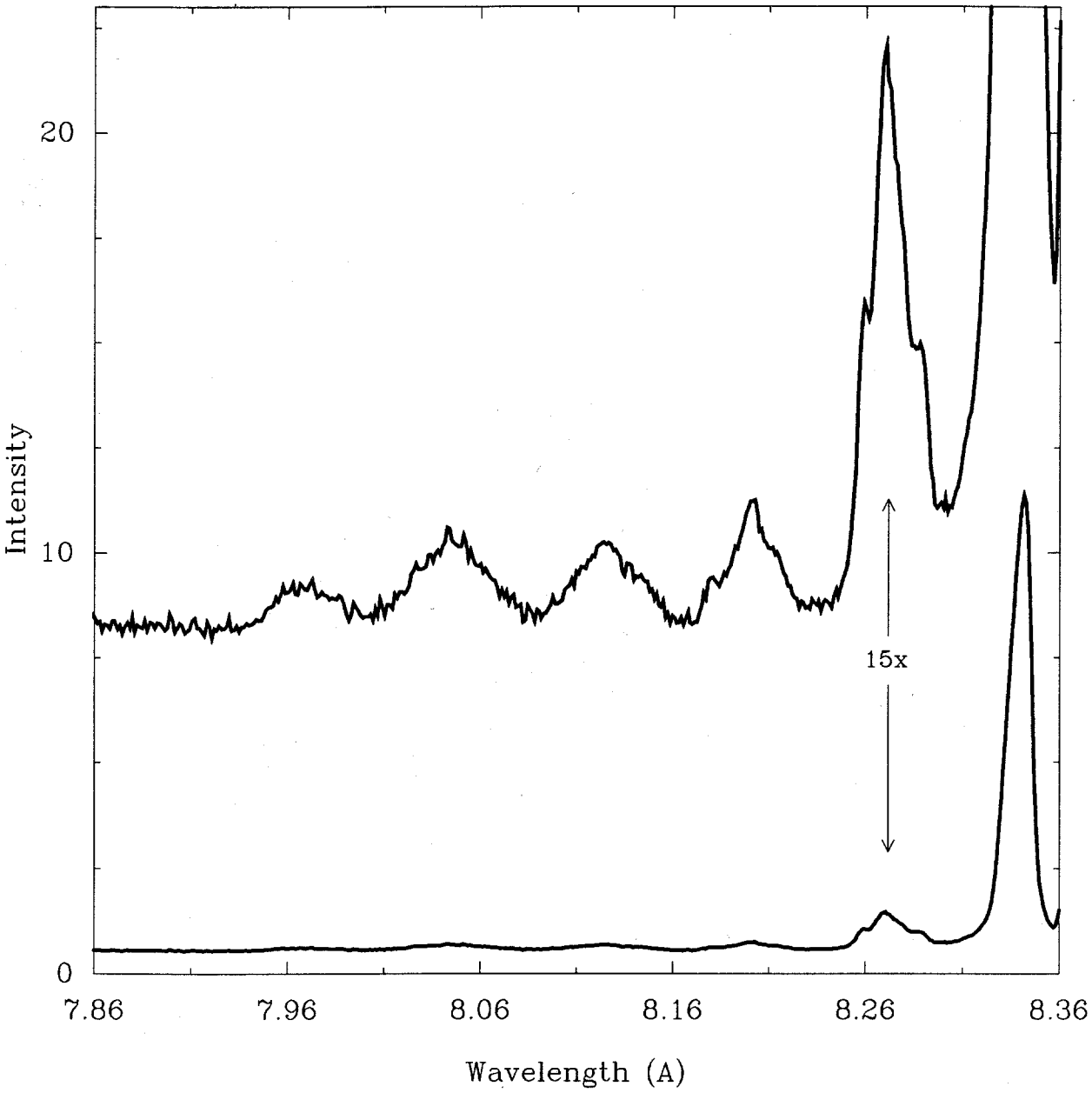

Figure 1. Kα spectrum from an aluminum target irradiated by the PBFA-II ion beam. The top spectrum is the same as the bottom spectrum, but with the amplitude multiplied by a factor of 15.

transitions involving the excited configuration states containing M-shell electrons because of the significant Stark broadening for these lines.

Detailed calculations of the wavelengths and transition probabilities of the Kα lines for aluminum ions has been carried out by Chenais-Popovics et al. [4] using a relativistic parametric potential method [5]. However, we found that some disagreements exist between their results and the PBFA-II experimental spectrum. This may be because the correlation effects were neglected in their calculation. To accurately compute wavelengths for transitions between the K- and L- shells of moderate-Z ions, both relativistic and correlation effects must be included in determining the transition energies. To date, the number of such relativistic configuration interaction (CI) calculations for the Kα transitions of aluminum ions is very small. Also, very few studies have been done for aluminum Kα satellite line structure with the inclusion of the transition involving the excited configuration states containing M- and higher shell electrons.

In the present study, configuration interaction calculations with Breit-Pauli relativistic corrections have been carried out for the Kα transitions of aluminum ions, including both the transitions involving the ground configuration states and those involving the low excited configuration states. The purpose of the calculations is to provide accurate transition energies and oscillator strengths for analyzing aluminum Kα spectra in light ion fusion experiments. In our calculations, we first performed multiconfiguration Hartree-Fock (MCHF) calculations [6] to determine a basis for the representation of the states of interest. Then a configuration-interaction calculation within the Breit-Pauli approximation was performed. In this way, both relativistic and correlation effects can be properly accounted for.

2. Calculations

All our calculations have been performed using the CI code CIBASE which is based on the modification of Fraga's configuration interaction program RIAS [7]. A brief overview of the calculation method used is given in this section.

The CI wavefunctions for each atomic state are represented by expansions of the form

$$\Psi(J, M_J) = \sum_{i}^{N} a_i \Phi(\alpha_i L_i S_i, J M_J) \tag{1}$$

where N is in principle infinite, but for all practical calculations is finite; $\{\Phi_i\}$ is a set of 'configuration wavefunctions' - each describing a configuration and is constructed from one-electron functions with $\{\alpha_i\}$ defining the coupling scheme of angular momenta of the electrons. The Hamiltonian matrix, with typical element $< \Phi_i|H|\Phi_j >$ can be diagonalized to give eigenvalues $E_1 < E_2 < \cdots < E_N$. Then from the Hylleraas-Undheim-MacDonald theorem [8], we have

$$E_k \geq E_k^{exact}\,. \tag{2}$$

The wavefunction associated with a particular eigenvalue (eigen-energy E_k) is then given by Eq. (1) with the $\{a_i\}$ taken to be the corresponding eigenvector components:

$$\sum_{j}^{N}(H_{ij} - E_k\delta_{ij})a_j = \ 0, \quad j = 1, 2, \ldots, N. \tag{3}$$

In the intermediate-coupling scheme the sum over i in the expansion includes N configurations in which the orbital L_i and spin S_i angular momenta couple to give the total angular momenta

$$J = L_i + S_i. \tag{4}$$

Each one-electron function is the product of a radial function, a spherical harmonic and a spin function. The configuration functions $\{\Phi_i\}$, and hence the eigenvalues $\{E_k\}$, depend on the choice of radial functions $\{P(nl|r)\}$. The inequalities of Eq. (2) allow any of the

eigenvalues to be used as the functional to be minimized with respect to variations in the radial functions. In this study, the multiconfiguration Hartree-Fock were performed using Froese Fischer's program MCHF77 [6]. The calcultions were carried out for the lowest state of each principal configuration under consideration, including configurations that involved all the orbitals to be used in the CI calculations. The radial functions obtained in such a way are ensured to be orthonormal automatically. It should be noted that we used the Breit-Pauli Hamiltonian only for determining the mixing coefficients a_i appearing in CI expansions and not for the optimization of the radial functions.

The Hamiltionian operator considered in this work may be written as

$$H = H_{el} + H_{SM} + H_{rel} \tag{5}$$

where H_{el} denotes the electronic Hamiltonian (consisting of the electron kinetic, nuclear attraction, and electrostatic repulsion energy terms), H_{SM} denotes the operator for specific mass effect, and

$$H_{rel} = H_{LS} + H_{fs} \tag{6}$$

includes the usual relativistic corrections: H_{LS} consists of the so-called LS-non-splitting terms (mass variation, Darwin corrections, and electron spin-spin contract and orbit-orbit interactions), H_{fs} includes the fine-structure (electron spin-own orbit, spin-other orbit and spin-spin dipole) couplings. Detailed expressions for each of these operators have been given in the literature [9,10].

Once wavefunctions in the form of Eq. (1) have been determined, they are used to obtain transition oscillator strengths for transitions between initial and final states Ψ^i and Ψ^j with energies E^i and E^j:

$$g_i f(i \rightarrow j) = \frac{2\Delta E}{3} | < \Psi^i | \sum_p \mathbf{r}_p | \Psi^j > |^2 \tag{7}$$

where $\Delta E = |E^i - E^j|$, $g_i = (2L_i + 1)(2S_i + 1)$ for L-S coupling and $g_i = 2J_i + 1$ for intermediate coupling.

3. Results And Discussion

3.1. Effects of correlation and relativistic corrections on the Kα transition energies

The salient feature of Kα transitions is the inclusion of K- and L-shell electrons. It is therefore important to examine the effects of both correlation and relativistic corrections on the Kα transition energies.

To study this problem, we have used four different approaches to calculate the transition energies for the term-dependent transitions of $1s^12s^22p^5 \rightarrow 1s^22s^22p^4$ and $1s^12s^12p^6 \rightarrow 1s^22s^12p^5$ in AlV (throughout the rest of this paper, the designation for ions is for the ionization stage before the K-shell ionization by proton impact): (1) nonrelativistic single-configuration Hartree-Fock (HF), (2) single-configuration Hartree-Fock with Breit-Pauli relativistic corrections (HF+BP), (3) nonrelativistic multiconfiguration Hartree-Fock (MCHF) and (4) configuration interaction with Breit-Pauli relativistic corrections (CI +BP). The calculated results are collected in Table I. Also given in Table I are the calculated values of Chenais-Popovics et al. The corresponding configurations used in the CI expansions are listed in Table II.

Two things should be noted in comparing the data in Table I. First, our HF+BP results are very close to those of Chenais-Popovics et al. This is because both calculations neglected the correlation effect but included the relativistic corrections. Second, if we take the results of CI+BP as a reference, it is easy to find that the wavelengths obtained from the MCHF calculation have a redshift while the wavelengths obtained from HF+BP calculation have a blueshift. The results of the HF calculation are closer to the results of the CI+BP than the others. In general, the relativistic effects are the strongest for inner-shell electrons, while the correlation effects are the strongest for outer atomic shells. Hence, it can be expected that the correlation corrections for the upper state ($1s^12s^22p^5$ and $1s^12s^12p^6$) energies are stronger than those for the lower state ($1s^22s^22p^4$ and $1s^22s^12p^5$) energies, and vice versa for the relativistic corrections. This is why

TABLE I

Calculated Wavelengths for the Term-Dependent Transitions of Al V

Transitions	HF	HF + BP	MCHF	CI + BP	Chenais-Popovics[4]
$1s^1 2s^2 2p^5 \rightarrow 1s^2 2s^2 2p^4$					
$^1P^\circ - {}^1S$	8.293	8.281	8.295	8.287	—
$^1P^\circ - {}^1D$	8.261	8.248	8.264	8.258	8.249
$^3P^\circ - {}^3P$	8.273	8.257	8.278	8.269	8.259
$1s^1 2s^1 2p^6 \rightarrow 1s^2 2s^1 2p^5$					
$^3S - {}^3P^\circ$	8.270	8.265	8.272	8.267	8.264
$^1S - {}^1P^\circ$	8.357	8.343	8.359	8.349	–

TABLE II

Configurations Used in the CI Expansions for Al V Calculations

$^1P^\circ$, $^3P^\circ$	^1S	^1D, ^3P
$1s^1 2s^2 2p^5$	$1s^2 2s^2 2p^4$	$1s^2 2s^2 2p^4$
$1s^1 2p^5 3s^2$	$1s^2 2p^6$	$1s^2 2p^4 3s^2$
$1s^1 2s^2 2p^3 3s^2$	$1s^2 2p^4 3s^2$	$1s^2 2s^2 2p^2 3s^2$
$1s^1 2s^2 2p^3 3p^2$	$1s^2 2s^2 2p^2 3s^2$	$1s^2 2s^2 2p^2 3p^2$
$1s^1 2s^2 2p^3 3d^2$	$1s^2 2s^2 2p^2 3p^2$	$1s^2 2s^2 2p^2 3d^2$
$1s^1 2s^2 2p^4 3p^1$	$1s^2 2s^2 2p^2 3d^2$	$1s^2 2s^2 2p^3 3p^1$
$1s^1 2s^2 2p^4 4f^1$	$1s^2 2s^2 2p^3 3p^1$	$1s^2 2s^2 2p^3 4f^1$
$1s^1 2s^1 2p^5 3d^1$	$1s^2 2s^1 2p^4 3d^1$	$1s^2 2s^1 2p^4 3d^1$

we can see a blueshift to the Kα transition energies when we included the relativistic corrections, while a redshift when we included the correlation corrections. Because the relativistic and correlational effects cause contrary shifts to the Kα transition energies, they cancel each other to some degree. Hence, the nonrelativistic single-configuration Hartree-Fock calculation can give reasonably good results. However, it must be noted that the relativistic corrections and the correlation correction do not cancel each other *exactly*. For the transitions considered here, the net adjustment to the wavelengths is about 4 - 6 mÅ. This suggests that to have reliable term-dependent Kα transition energies, both relativistic and correlation effects should be properly accounted for.

Figure 2 shows a comparison of the calculated wavelengths of CI+BP for AlV Kα satellites and the PBFA-II experimental data. The three features in the AlV satellites are attributed to the term-dependent transitions of $1s^1 2s^2 2p^5 \rightarrow 1s^2 2s^2 2p^4$ and $1s^1 2s^1 2p^6 \rightarrow 1s^2 2s^1 2p^5$. Very good agreement is achieved. The good agreement between the calculated wavelengths and experimental data allows us to determine with confidence transitions responsible for peaks in an experimental spectrum.

3.2. Structure of the Kα satellites of aluminum ions

Kα radiation in light ion beam experiments is emitted as a result of two processes: ion-impact ionization of a 1s electron followed by a spontaneous fluorescence transition, while the shift of the Kα satellite lines is produced by removing electrons from the L shell. Electrons can be removed from the L shell by both ionization and excitation of thermal electrons and ion beams. For the aluminum plasma considered here, the effect of ionization and excitation of L-shell electrons by ion beams is much smaller than that by thermal electrons because of the lower values of ion impact cross sections. It should be noted the ionization process not only removes an electron from the L shell but also introduces a new ionization stage. In other words, Kα satellite lines shifted by ionization and those shifted by excitation represent two different ionization stages.

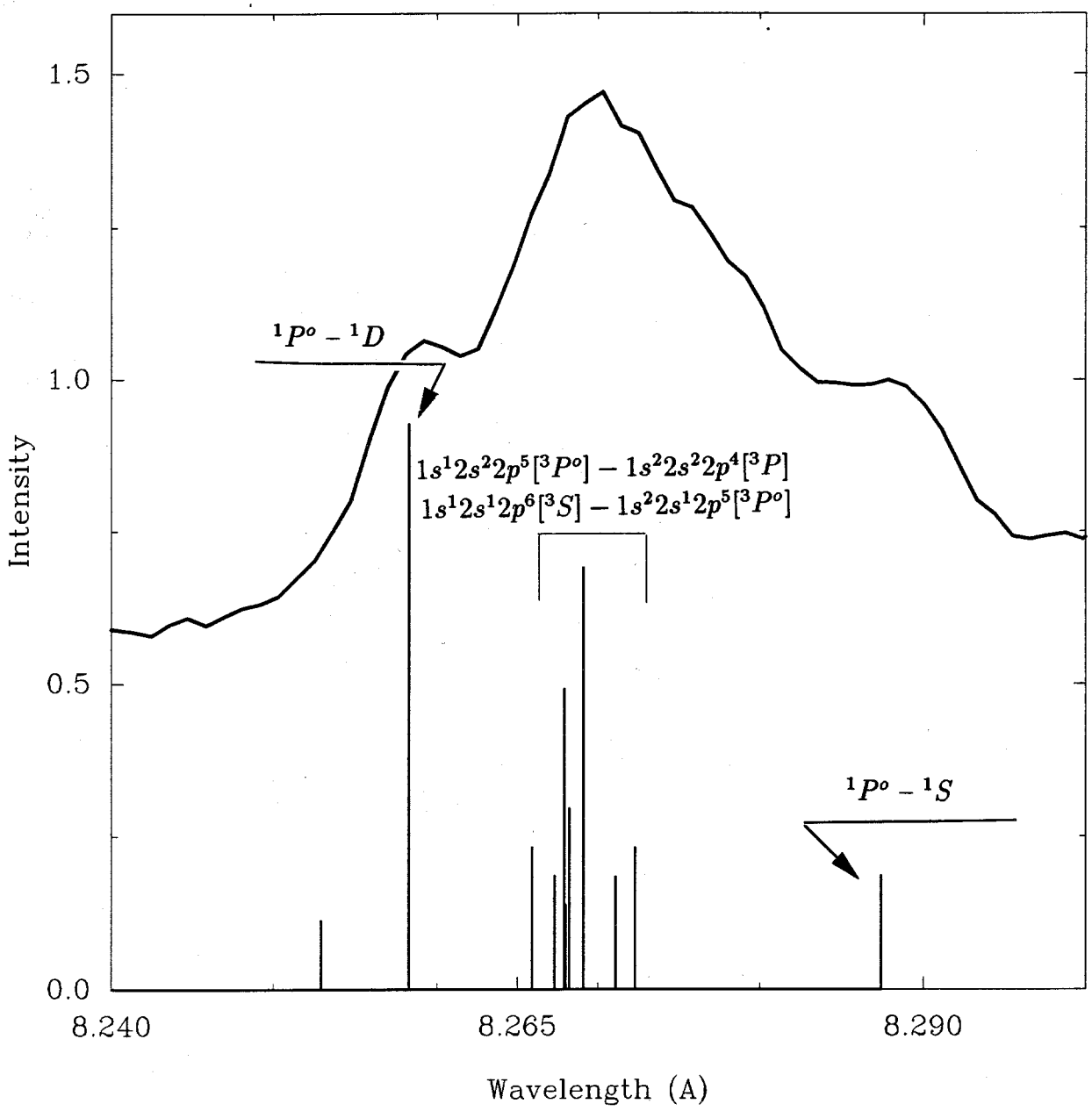

Figure 2. Comparison of the calculated wavelengths and relative intensities (gf) with the PBFA-II experimental data. The stick spectrum represents the lines associated with the transitions $1s^12s^22p^5 \rightarrow 1s^22s^22p^4$ and $1s^12s^12p^6 \rightarrow 1s^22s^12p^5$.

Let us look at the processes of Kα emission from ions with one L shell hole created by thermal ionization and excitation in a proton beam heated Al plasma:

$$1s^2 2s^2 2p^6 \overset{thermal\ ionization}{\longrightarrow} 1s^2 2s^2 2p^5 \tag{8}$$

$$1s^2 2s^2 2p^5 \overset{beam\ ionization}{\longrightarrow} 1s^1 2s^2 2p^5 \overset{K\alpha\ fluorescence\ decay}{\longrightarrow} 1s^2 2s^2 2p^4 \tag{9}$$

$$1s^2 2s^2 2p^6 \overset{thermal\ excitation}{\longrightarrow} 1s^2 2s^2 2p^5 nl^1 \tag{10}$$

$$1s^2 2s^2 2p^5 nl^1 \overset{beam\ ionization}{\longrightarrow} 1s^1 2s^2 2p^5 nl^1 \overset{K\alpha\ fluorescence\ decay}{\longrightarrow} 1s^2 2s^2 2p^4 nl^1 \tag{11}$$

For ions with the L shell being an outer shell, if the thermal ionization process in (8) is important, it can be expected that the thermal excitation process in (10) will be appreciable. Hence, to interpret the structure of a Kα satellite line spectrum of a plasma, it is necessary to include the contributions of the transitions involving the excited configuration states of type $1s^1 2s^2 2p^N nl^1$.

We first consider the Kα transitions of AlI to AlIII, i.e., the Kα lines of those ions with no holes in the L shell and with spectator electrons in the M shell. For these ions, the L shell is not an outer shell. It is expected that the transitions involving the excited configuration states with a $2p$ electron excited to the M shell have little contribution to the Kα satellite line spectra. Hence, we only considered the Kα transitions involving ground configuration states, i.e., the transitions of type:

$$1s^1 2s^2 2p^6 3l^N \longrightarrow 1s^2 2s^2 2p^5 3l^N. \tag{12}$$

The calculated wavelengths and gf values of Kα lines are given in Table III. The corresponding stick spectrum is given in Figure 3. It can be seen that the effect of removing electrons from the M shell on the Kα lines is relatively unimportant as the corresponding energy shifts of Kα transitions from AlI to AlIII are small. The Kα lines cover a rather small range from 8.325 Å to 8.340 Å. By comparing with the PBFA-II

TABLE III

Calculated Wavelengths and gf Values for the
Characteristic Kα Lines from Al I to Al IV

Ion	Transition				Wavelength (Å)	gf
Al I	$1s^2 2s^2 2p^5 3s^2 3p^1$	$[^3D_1]$ –	$1s^1 2s^2 2p^6 3s^2 3p^1$	$[^3P_\circ]$	8.3373	0.163
		$[^3P_1]$ –		$[^3P_2]$	8.3399	0.104
		$[^3S_1]$ –		$[^3P_2]$	8.3329	0.103
		$[^1P_1]$ –		$[^1P_1]$	8.3374	0.113
		$[^3D_2]$ –		$[^3P_1]$	8.3365	0.326
		$[^3P_2]$ –		$[^1P_1]$	8.3379	0.167
		$[^1D_2]$ –		$[^1P_1]$	8.3363	0.196
		$[^3P_2]$ –		$[^3P_2]$	8.3396	0.246
		$[^1D_2]$ –		$[^3P_2]$	8.3380	0.135
		$[^3D_3]$ –		$[^3P_2]$	8.3359	0.578
Al II	$1s^2 2s^2 2p^5 3s^2$	$[^2P_{1/2}]$ –	$1s^1 2s^2 2p^6 3s^2$	$[^2S_{1/2}]$	8.3369	0.164
		$[^2P_{3/2}]$ –		$[^2S_{1/2}]$	8.3346	0.328
Al III	$1s^2 2s^2 2p^5 3s^1$	$[^3P_1]$ –	$1s^1 2s^2 2p^6 3s^1$	$[^3S_1]$	8.3321	0.237
		$[^3P_2]$ –		$[^3S_1]$	8.3298	0.431
		$[^1P_1]$ –		$[^1S_1]$	8.3303	0.235
Al IV	$1s^2 2s^2 2p^5$	$[^2P_{1/2}]$ –	$1s^1 2s^2 2p^6$	$[^2S_{1/2}]$	8.3270	0.173
		$[^2P_{3/2}]$ –		$[^2S_{1/2}]$	8.3256	0.346

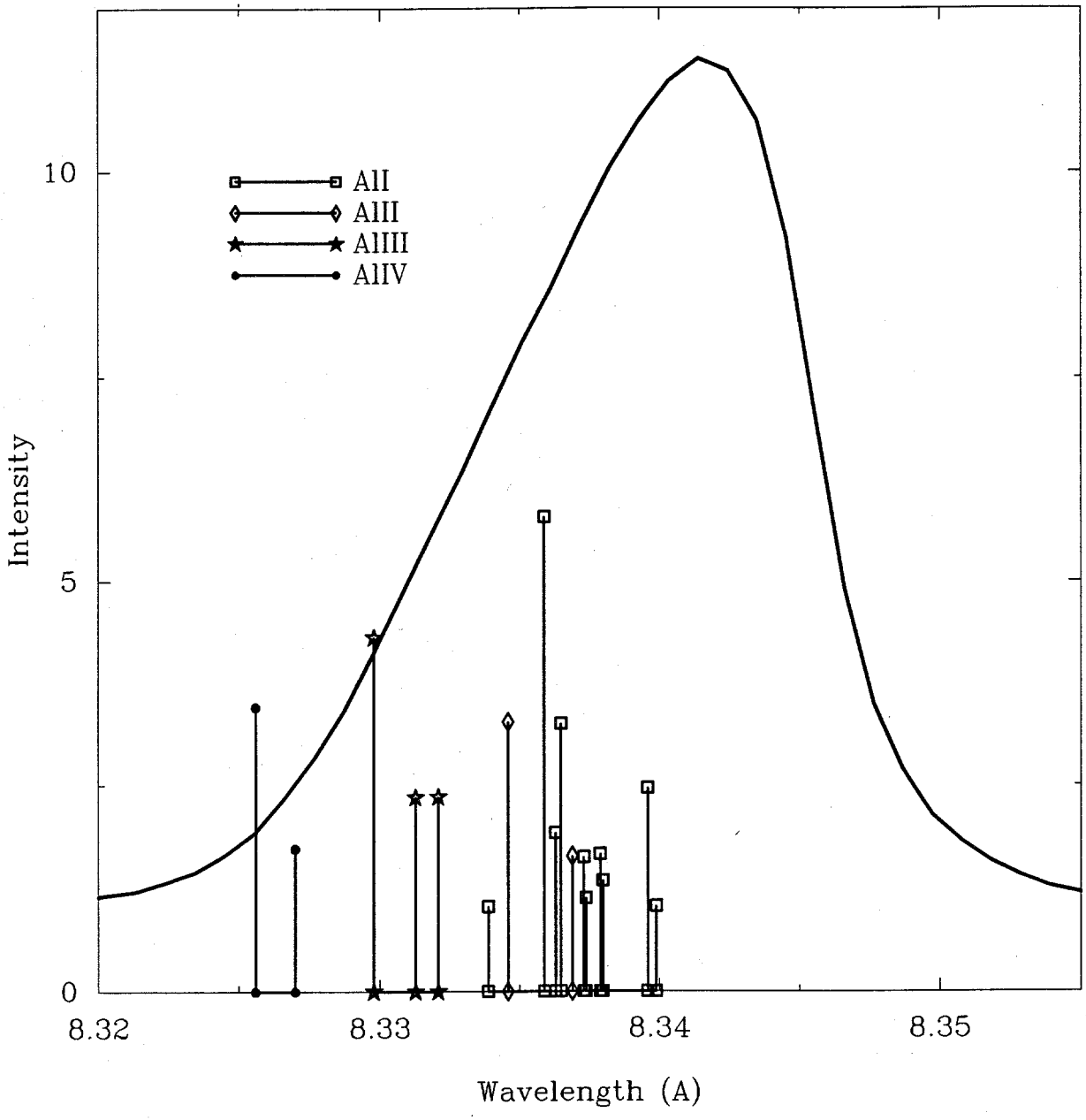

Figure 3. Kα lines for the transitions involving ground configuration states from AlI to AlIV. The broad line is the PBFA-II experimental spectrum.

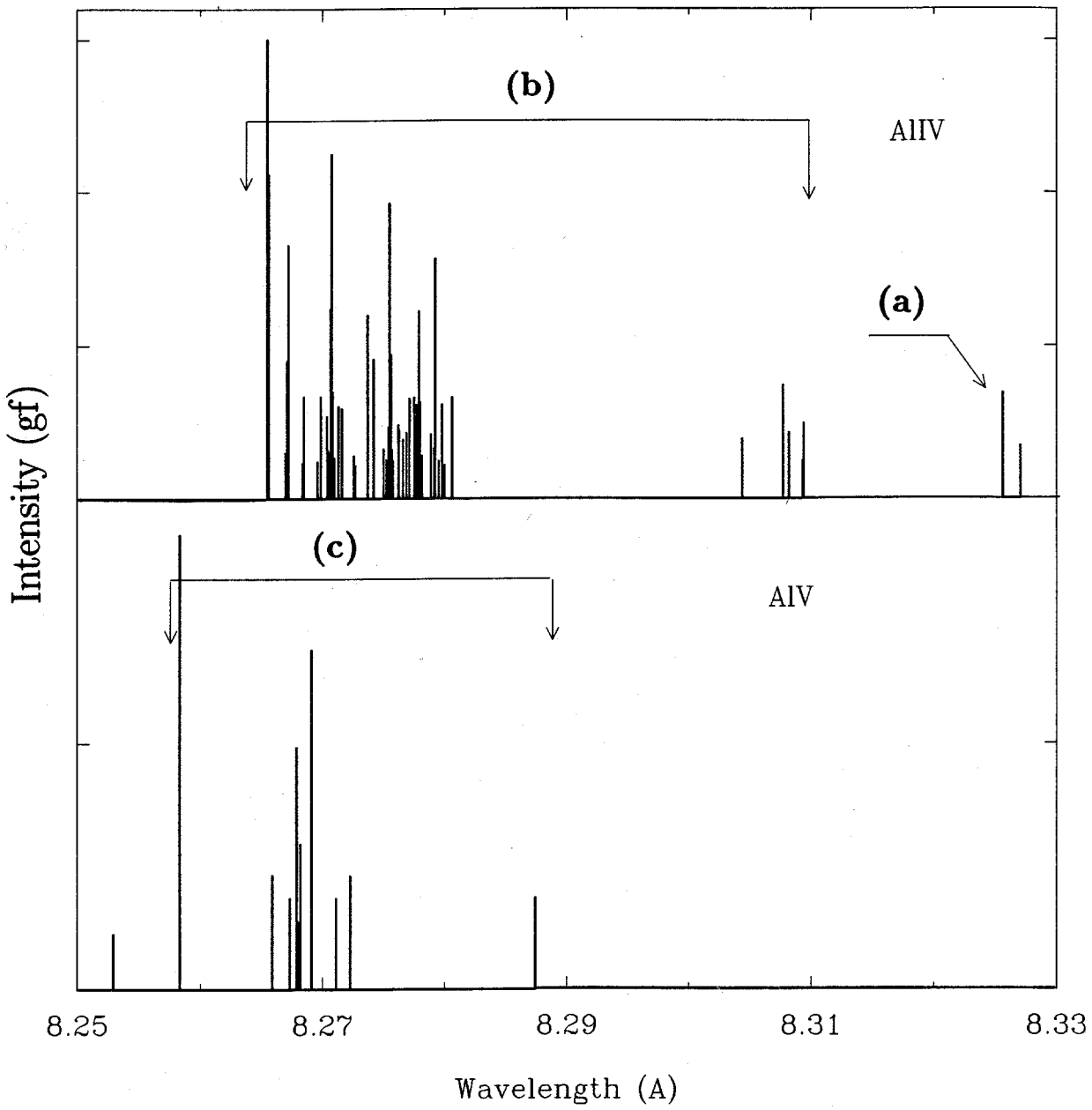

Figure 4. Calculated wavelengths and relative intensities of Kα satellite lines from AlIV and AlV. The lines are classified into groups: (a) $1s^1 2s^2 2p^6 \rightarrow 1s^2 2s^2 2p^5$, (b) $1s^1 2s^2 2p^5 3l^1 \rightarrow 1s^2 2s^2 2p^4 3l^1$, and (c) $1s^1 2s^2 2p^5 \rightarrow 1s^2 2s^2 2p^4$ and $1s^1 2s^1 2p^6 \rightarrow 1s^2 2s^1 2p^5$.

experimental spectrum, these Kα satellite lines are unresolvable and give a broad line which is asymmetric toward the short wavelength side.

In the case of AlIV, there are no holes in the L shell in the ground configuration. Two Kα lines are associated with the transition

$$1s^1 2s^2 2p^6 \longrightarrow 1s^2 2s^2 2p^5. \tag{13}$$

Our calculation shows that these two lines overlap the wavelength range of AlI-AlIII. On the other hand, when the L shell is an outer shell, an L shell hole can be easily produced by exciting a 2p electron to the M shell. In this case, we have Kα lines related to the transition group

$$1s^1 2s^2 2p^5 3l^1 \longrightarrow 1s^2 2s^2 2p^4 3l^1, \tag{14}$$

where l represents the s, p, or d subshell. There are about two hundred lines associated with this transition group. The calculated line positions and the corresponding oscillator strengths for these Kα lines will be published elsewhere [11]. In Figure 4, we present the stick spectrum of Kα lines for AlIV, along with the Kα lines for the transitions $1s^1 2s^2 2p^5 \rightarrow 1s^2 2s^2 2p^4$ and $1s^1 2s^1 2p^6 \rightarrow 1s^2 2s^1 2p^5$ of AlV. As shown, the structure of Kα satellite lines for the transition group of $1s^1 2s^2 2p^5 3l^1 \rightarrow 1s^2 2s^2 2p^4 3l^1$ is very complex. These satellite lines are blueshifted with respect to the Kα lines of the ground configuration states of AlIV and strongly overlap the Kα lines of AlV. The blueshift effect is caused by the reduced screening of the nucleus, which results when a 2p electron is excited to the M shell or a higher shell. The overlap effect is because the valence electron in M or a higher shell has little effect on the electronic wavefunctions in the inner regions of the ion, and therefore the effect of removing an electron from the M shell on Kα transition energies is very small. Hence there is no significant shift from $1s^1 2s^2 2p^5 3l^1 \rightarrow 1s^2 2s^2 2p^4 3l^1$ to $1s^1 2s^2 2p^5 \rightarrow 1s^2 2s^2 2p^4$. This overlap phenomenon of Kα lines of AlIV and AlV may partially explain why the central peak of AlV lines in the PBFA-II experimental spectrum is asymmetric toward the long wavelength side.

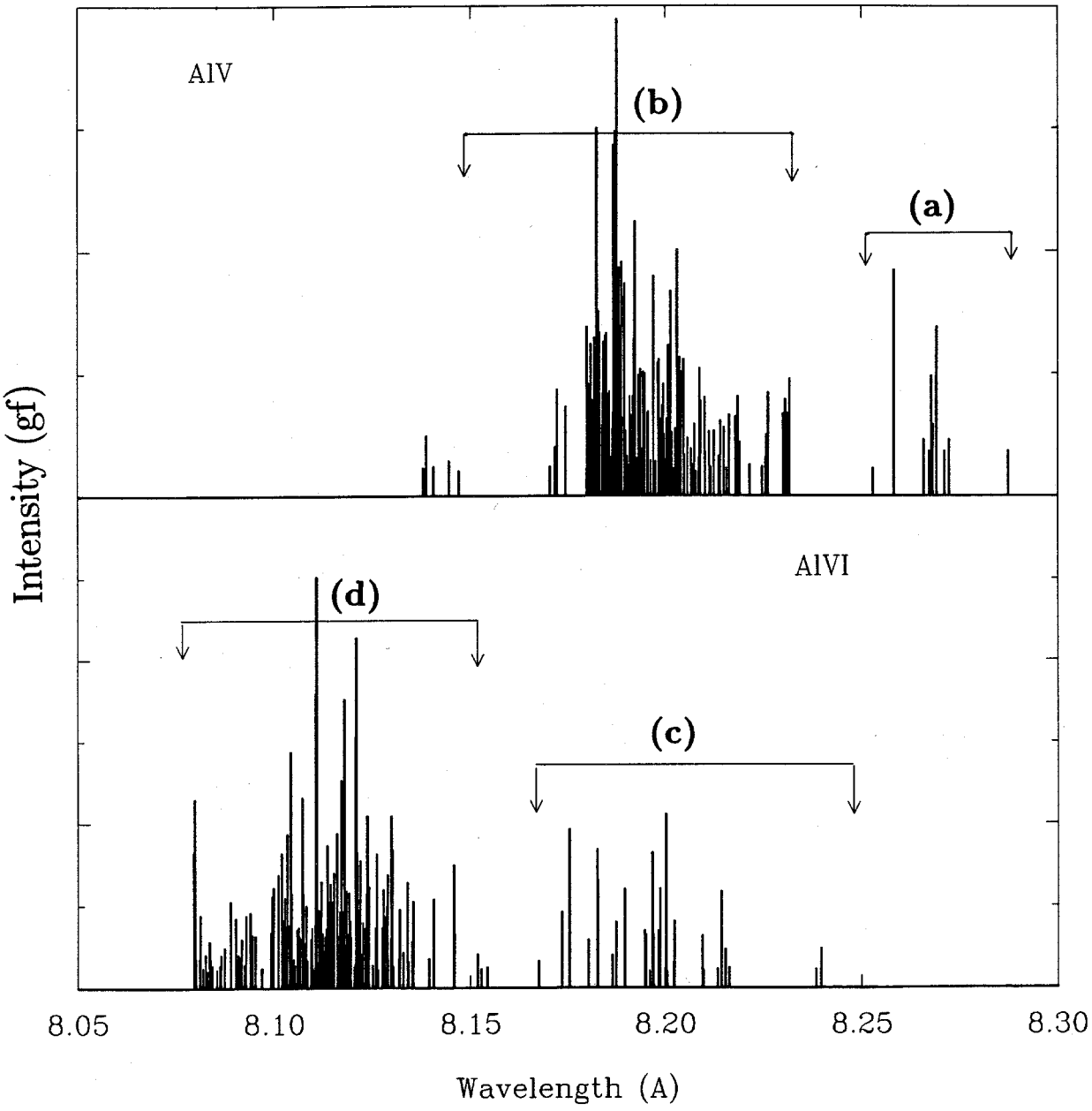

Figure 5. Calculated wavelengths and relative intensities of Kα satellite lines from AlV and AlVI. The lines are classified into groups: (a) $1s^1 2s^2 2p^5 \rightarrow 1s^2 2s^2 2p^4$ and $1s^1 2s^1 2p^6 \rightarrow 1s^2 2s^1 2p^5$, (b) $1s^1 2s^2 2p^4 3l^1 \rightarrow 1s^2 2s^2 2p^3 3l^1$, (c) $1s^1 2s^M 2p^N \rightarrow 1s^2 2s^M 2p^{N-1}$, and (d) $1s^1 2s^2 2p^3 3l^1 \rightarrow 1s^2 2s^2 2p^2 3l^1$.

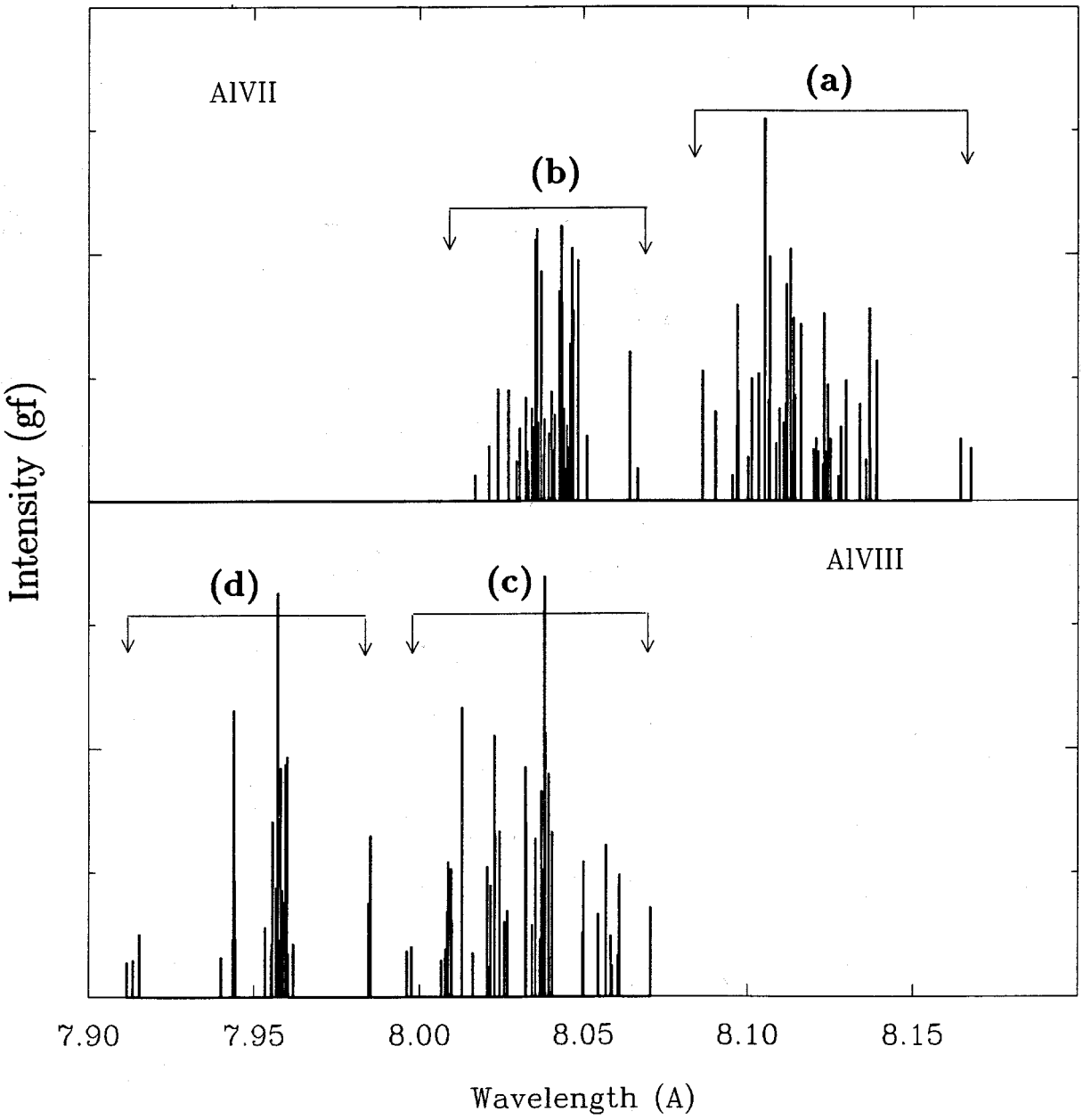

Figure 6. Calculated wavelengths and relative intensities of Kα satellite lines from AlVII and AlVIII. The lines are classified into groups: (a) $1s^1 2s^M 2p^N \rightarrow 1s^2 2s^M 2p^{N-1}$, (b) $1s^1 2s^2 2p^2 3l^1 \rightarrow 1s^2 2s^2 2p^1 3l^1$, (c) $1s^1 2s^M 2p^N \rightarrow 1s^2 2s^M 2p^{N-1}$, and (d) $1s^1 2s^2 2p^1 3l^1 \rightarrow 1s^2 2s^2 3l^1$.

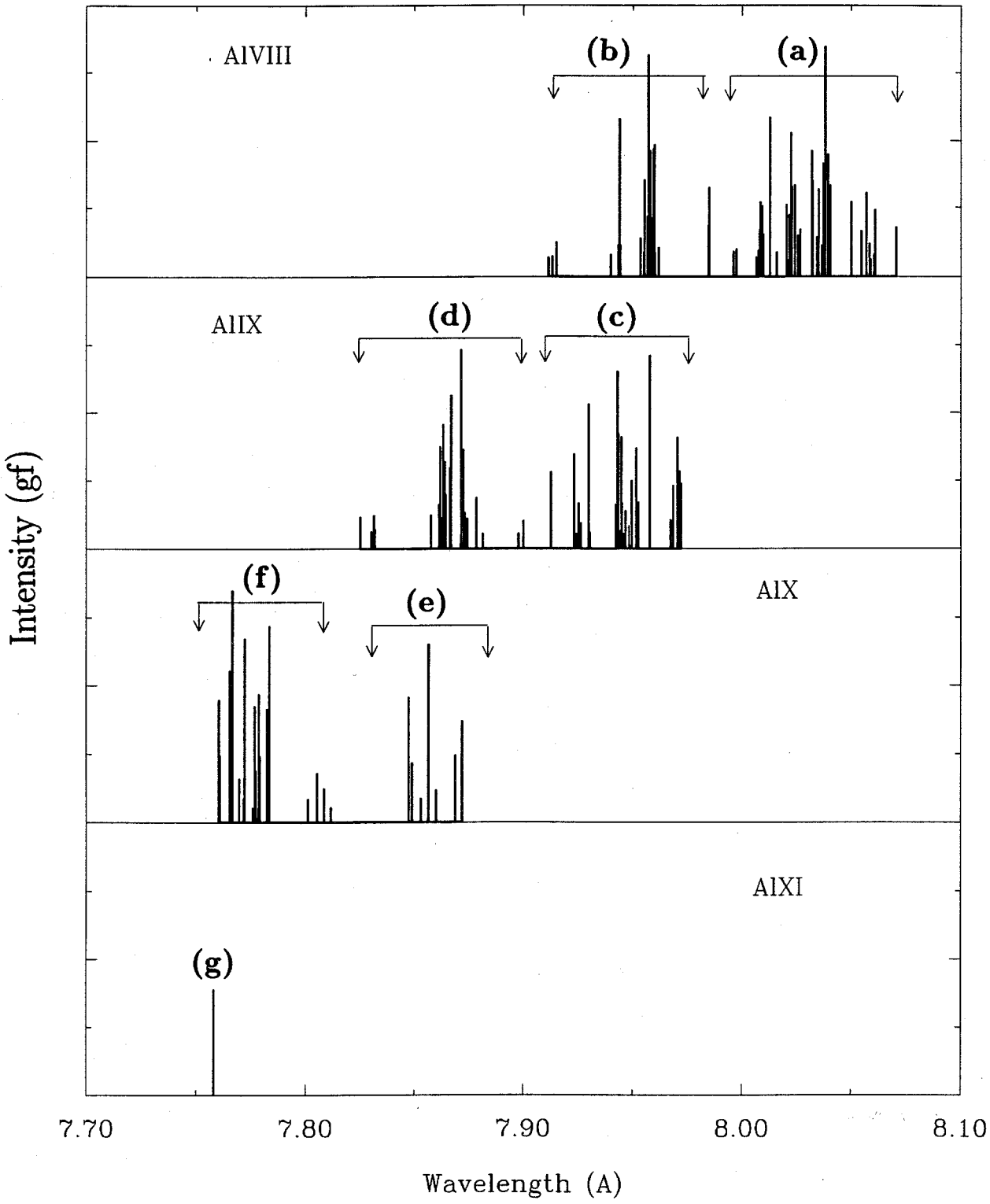

Figure 7. Calculated wavelengths and relative intensities of Kα satellite lines from AlVIII to AlXI. The lines are classified into groups as shown.

Our calculation shows that this overlap phenomenon also appears for other ions in higher ionization stages. All the calculated results are summarized in Figure 5, Figure 6, and Figure It can be seen from the figures that the Kα lines for a specific ionization stage can be classified into two groups. One is the 'characteristic group', which represents the characteristic Kα line position of the ionization stage. The Kα lines of this group are from the transitions involving the ground configuration states and the transitions involving excited configuration states with a 2s electron excited to a 2p subshell. Another is the 'overlap group', which overlaps the characteristic Kα lines of the next higher ionization stage and affects the whole characteristic line shape. The Kα lines of this group are from the transitions involving the excited configuration states with a 2p electron excited to the M shell or a higher shell. This overlap phenomenon of Kα lines of two consecutive ionization stages is important for the spectroscopy analysis of Kα satellite spectra. It has been found [3,12] that the Stark broadening effect for the lines in the overlap group is much stronger than that for the lines in the characteristic group. In a plasma of moderate to high density, the lines in overlap groups show a much more pronounced dependence on electron density than those in characteristic groups. Thus, the Kα lines in overlap groups offer better opportunities for diagnosing plasma densities.

In Figure 8, we present a stick spectrum which includes the Kα lines of AlI to AlXI and compare with the PBFA-II experimental spectrum. It can be seen that the overlap effect of the Kα satellite lines of two consecutive ionization stages plays an important role for the broad feature of the Kα satellite lines in the experimental spectrum. Other effects, such as the opacity effect and time integration effect, can also have contributions to the broad line shape. Detailed discussions of these effects have been given elsewhere [12]. Our calculation also shows that the peak with the shortest wavelength in the experimental spectrum is actually attributed to the Kα transitions of ground configuration states of AlIX, excited states of AlVIII, and the Kβ transition of AlI.

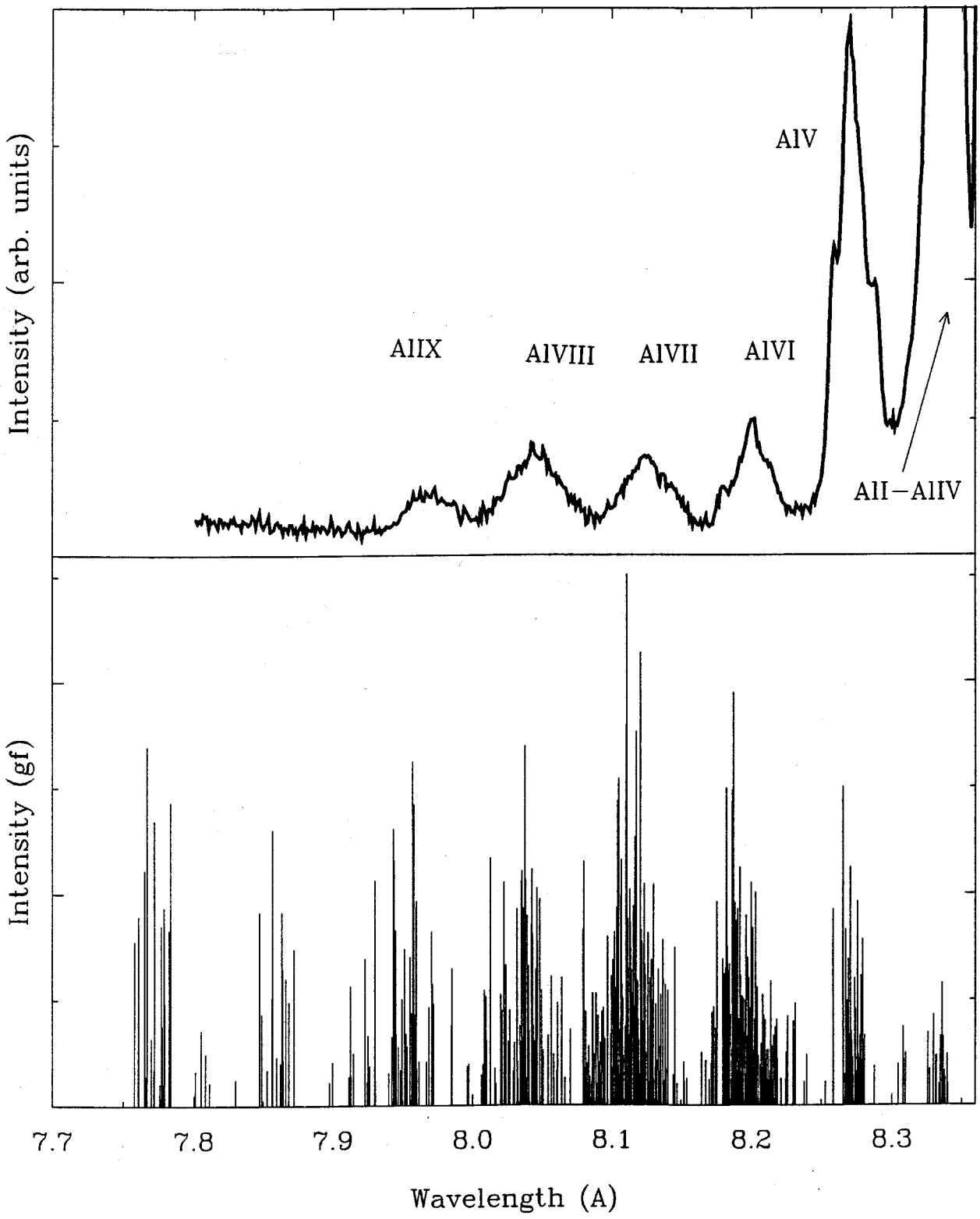

Figure 8. Theoretically calculated Kα satellite spectrum of aluminum. Upper: PBFA-II experimental Kα spectrum.

4. Conclusions

In order to analyze the experimental aluminum Kα spectrum of a PBFA-II experiment, it is necessary to understand the detailed structure of Kα satellite lines of aluminum ions. In this paper, we have used the CI+BP method to calculate the transition energies and oscillator strengths for the Kα transitions of aluminum ions. Our calculated wavelengths for the most prominant Kα transitions agree well with the PBFA-II experimental data. In particular, we have calculated the properties for Kα lines involving excited configuration states. It has been found from our calculations that for ions with the L shell being an outer shell (AlIV to AlXI), the corresponding Kα satellite lines can be classified into 'characteristic' and 'overlap' groups. The 'characteristic' group, which is associated with the lines of transitions involving ground configuration states, can be used for characterizing the ionization stage, while the 'overlap' group, which is associated with the Kα lines of transitions involving excited configuration states with a 2p electron excited to the M shell or higher shells, can have important effects on the line shape of Kα satellite lines.

Our calculated results have been used to simulate the Kα experimental spectrum of a PBFA-II experiment with a collisional-radiative-equilibrium (CRE) model post-processed by hydrodynamics simulations. Good agreement with the experimental spectrum is achieved. The simulation results are described elsewhere [12].

Acknowledgements

This work has been supported in part by the Sandia National Laboratories and by Kernforschungszentrum Karlsruhe (FRG) through Fusion Power Associates. Computing support was provided in part by the National Science Foundation through the San Diego Supercomputer Center.

References

1. E. Nardi, Z. Zinamon, *J. Appl. Phys.* **52**, 7075 (1981).

2. J. Bailey, A.L. Carlson, G. Chandler, M.S. Derzon, R.J. Dukart, B.A. Hammel, D.J. Johnson, T.R. Lockner, J. Maenchen, E.J. McGuire, T.A. Mehlhorn, W.E. Nelson, L.E. Ruggles, W.A. Stygar, and D.F. Wenger, *Lasers and Particle Beams* **8**, 555 (1990).

3. R. Mancini, *Priviate Communication*, (1991).

4. C. Chenais-Popovics, C. Fievet, J.P. Geindre, and J.C. Gauthier, *Phys. Rev.* **40**, 3194 (1989).

5. M. Klapisch, J.L. Schwob, B.S. Fraenkel, and J. Oreg, *J. Opt. Soc. Am.* **67**, 148 (1977).

6. C.F. Fischer, *Comp. Phys. Commun.* **14**, 145 (1978).

7. S. Fraga, M. Klobukowski, J. Muszynsha, K.M.S. Saxena, J.A. Sordo, and J.D. Climenhaga, *Comp. Phys. Commun.* **47**, 159 (1987).

8. J.F. Perkins, *J. Chem. Phys.* **45**, 2156 (1965).

9. R. Glass, A. Hibbert, *Comp. Phys. Commun.* **16**, 19 (1978).

10. S. Fraga, M. Klobukowski, J. Muszynsha, K.M.S. Saxena, and J.A. Sordo, *Phys. Rev.* **34**, 23 (1986).

11. P. Wang, J.J. MacFarlane, and G.A. Moses, *Atomic Data and Nuclear Data Tables*, to be submitted (1992).

12. J.J. MacFarlane, P. Wang, J. Bailey, T.A. Mehlhorn, R.J. Dukart, and R. Mancini, *Phys. Rev.* submitted (1992).